


Emergence of Boltzmann Subspaces in Open Quantum Systems Far from Equilibrium

Michael Iv¹, Saar Rahav¹, and Uri Peskin^{1,2}

¹*Schulich Faculty of Chemistry, Technion-Israel Institute of Technology, Haifa 32000, Israel*
²*The Helen Diller Quantum Center, Technion-Israel Institute of Technology, Haifa 32000, Israel*

 (Received 26 January 2023; accepted 5 February 2024; published 15 March 2024)

Single molecule junctions are important examples of complex out-of-equilibrium many-body quantum systems. We identify a nontrivial clustering of steady state populations into distinctive subspaces with Boltzmann-like statistics, which persist far from equilibrium. Such Boltzmann subspaces significantly reduce the information needed to describe the steady state, enabling modeling of high-dimensional systems that are otherwise beyond the reach of current computations. The emergence of Boltzmann subspaces is demonstrated analytically and numerically for fermionic transport systems of increasing complexity.

DOI: 10.1103/PhysRevLett.132.110401

Understanding complex many-body quantum systems out of equilibrium is fundamentally challenging [1–6] as well as crucial for the design and optimization of quantum devices (quantum computers, switches, sensors, etc.). Generic examples that attracted much attention recently are molecular junctions, in which a single molecule is coupled to two electrodes (fermion reservoirs) under a potential bias [7–12]. The field of molecular electronics is developing rapidly due to experimental realizations of controllable single molecule junctions [12–22] and theoretical ideas for new functionality [23–33]. Especially promising are experiments where the molecule obtains a nonequilibrium steady state which substantially differs from its well-understood equilibrium state. For example, assigning a global temperature to a molecular junction is often irrelevant, and the concept of a local temperature [34–36], or the assignment of different temperatures to different degrees of freedom [27,37–39] becomes instrumental.

Various theoretical approaches can be used to describe such open quantum systems [40–43]. These often exhibit a tradeoff between level of detail and practicability. Approximate methods such as the NEGF-DFT framework can account for details of electronic and vibronic interactions [44,45]. Impurity models [46–48] enable numerically exact computations [49–59] of many-body dynamics, but only for small systems. Markovian approximations can greatly simplify the description of systems that are weakly coupled to reservoirs [40,41], where the dissipative dynamics follows Redfield or Lindblad equations [42,60]. When the bath-induced dynamics is (comparatively) slow these simplify to Pauli master equations [40,41]. Crucially, while being conceptually straightforward, the solution of master equations is still highly demanding when the dimensions of Hilbert (or Fock) space become large [61]. These dimensions can become notoriously high in polyatomic molecules and supramolecular structures [62,63]. It is therefore

desirable to develop a theory that describes such high-dimensional systems in the simplest possible way.

In this work we present an approach that allows to reduce the complexity of nonequilibrium steady state calculations in such systems. The approach is based on the emergence of “equilibrated” subspaces, whose eigenstate populations have the form $P_n(\tau) \cong P^{(N)}(\tau)B_{N,n}$, where the internal distribution within each subspace, $\{B_{N,n}\}$ is known (with $\sum_{n \in N} B_{N,n} = 1$). Once such subspaces are identified, the steady state probabilities to be in each subspace can be calculated using $(\partial/\partial\tau)P^{(N)}(\tau) = \sum_{N'} k_{N' \rightarrow N} P^{(N')}(\tau) - k_{N \rightarrow N'} P^{(N)}(\tau) = 0$, with $k_{N' \rightarrow N} \equiv [\sum_{n \in N} \sum_{n' \in N'} k_{n' \rightarrow n} B_{N',n'}]$. The dimension of the kinetic equations is therefore reduced to the number of subspaces.

We demonstrate the usefulness of this approach, conceptually and computationally, for several models, where we identify subspaces with $B_{N,n} \cong c_N e^{(-E_n/k_B T)}$, which we term “Boltzmann subspaces.” This allows to interpret $\{k_{N' \rightarrow N}\}$ as “thermal rate constants” [41] for transitions between the subspaces. Such subspaces are often indicative of separation of timescales, with fast intraspace relaxation, and slow interspace transitions. Remarkably, we also find such subspaces in far from equilibrium steady states without evident timescale separation.

Our basic model includes a system of fermions with the Hamiltonian, $\hat{H}_S = \sum_{m=1}^M \varepsilon_m \hat{a}_m^\dagger \hat{a}_m + \frac{1}{2} \sum_{i,j,k,l=1}^M w_{ijkl} \hat{a}_i^\dagger \hat{a}_j^\dagger \hat{a}_l \hat{a}_k$. Here \hat{a}_m^\dagger creates an electron in the m th single particle state (spin-orbital) at energy ε_m , and $\{w_{ijkl}\}$ are the standard Coulomb interaction terms. When \hat{H}_S commutes with all the orbital number operators, each eigenstate is characterized by an occupation vector, $\mathbf{n} = (n_1, n_2, \dots, n_M)$, where $n_m \in 0, 1$ corresponds to the occupation of the m th spin orbital, which defines the state’s energy ($\hat{H}_S|\mathbf{n}\rangle = E_{\mathbf{n}}|\mathbf{n}\rangle$) and total electron number ($\sum_{m=1}^M \hat{a}_m^\dagger \hat{a}_m |\mathbf{n}\rangle = N_{\mathbf{n}}|\mathbf{n}\rangle$). The system is weakly coupled

to two reservoirs of noninteracting fermions, associated with equilibrium densities, $\hat{\rho}_K = (1/Z_K)e^{-\beta(\hat{H}_K - \mu_K \hat{N}_K)}$, where $K \in \{R, L\}$ marks the right or left reservoir with, $\hat{H}_K = \sum_{k_K} \varepsilon_{k_K} \hat{b}_{k_K}^\dagger \hat{b}_{k_K}$ and $\hat{N}_K = \sum_{k_K} \hat{b}_{k_K}^\dagger \hat{b}_{k_K}$. μ_K and Z_K are the chemical potential and partition function, and $\beta = (1/k_B T)$. The full Hamiltonian reads, $\hat{H} = \hat{H}_S + \sum_{K \in \{R, L\}} \{\hat{H}_K + [\hat{V}_K \otimes \hat{U}_K + \text{H.c.}]\}$, where $\hat{V}_K (\hat{U}_K)$ is the system (reservoir) electronic coupling operator, with $\hat{V}_K = \sum_{m=1}^M \lambda_{m,K} \hat{a}_m^\dagger$ and $\hat{U}_K = \sum_{k_K} \xi_{k_K} \hat{b}_{k_K}$. Under weak coupling [41], the reservoirs induce changes in the eigenstate populations, corresponding to electron absorption ($k_{\mathbf{n}' \rightarrow \mathbf{n}}^{(K)} = \delta_{\mathbf{n}' - \mathbf{n}, \mathbf{e}_m} |\langle \mathbf{n}' | \hat{V}_K | \mathbf{n} \rangle|^2 \Gamma_K(\varepsilon_m) f_{K,m} / \hbar$) and emission ($k_{\mathbf{n}' \rightarrow \mathbf{n}}^{(K)} = \delta_{\mathbf{n}' - \mathbf{n}, \mathbf{e}_m} |\langle \mathbf{n}' | \hat{V}_K | \mathbf{n} \rangle|^2 \Gamma_K(\varepsilon_m) (1 - f_{K,m}) / \hbar$) rates, where $f_{K,m} \equiv 1 / (1 + e^{(\varepsilon_m - \mu_K) / (k_B T)})$ is the Fermi distribution, and $\mathbf{e}_m = (\delta_{m,1}, \delta_{m,2}, \dots, \delta_{m,M})^t$. Here $\Gamma_K(\varepsilon) = 2\pi \sum_{k_K} |\xi_{k_K}|^2 \delta(\varepsilon - \varepsilon_{k_K})$ is the reservoir spectral density.

When accounting for coupling to (external or internal) bosonic reservoirs in the weak coupling limit, additional changes in the system eigenstate populations are induced, corresponding to energy absorption ($k_{\mathbf{n}' \rightarrow \mathbf{n}}^{(B)} = \sum_{n_b=1}^N |\langle \mathbf{n}' | \hat{V}_{n_b} | \mathbf{n} \rangle|^2 [J_{n_b}(E_n - E_{\mathbf{n}'}) / \hbar] B_{n_b}(E_n - E_{\mathbf{n}'})$) or emission ($k_{\mathbf{n}' \rightarrow \mathbf{n}}^{(B)} = \sum_{n_b=1}^N |\langle \mathbf{n}' | \hat{V}_{n_b} | \mathbf{n} \rangle|^2 [J_{n_b}(E_{\mathbf{n}'} - E_n) / \hbar] [1 + B_{n_b}(E_{\mathbf{n}'} - E_n)]$) rates, where \hat{V}_{n_b} is the system coupling operator to the n_b reservoir, $J_{n_b}(E)$ is the respective reservoir spectral density and $B_{n_b}(E) = 1 / (e^{E / (k_B T)} - 1)$ is the Bose-Einstein distribution.

At equilibrium, the two electrodes share the same chemical potential, $\mu_L = \mu_R = \mu$, and the same temperature. Consequently, a system of fermions (interacting or not), weakly coupled to the electrodes, obtains the

reduced density,

$$\hat{\rho}_S = \frac{1}{Z_S} e^{-\beta(\hat{H}_S - \mu \hat{N}_S)}; \quad Z_S = \text{tr} \{ e^{-\beta(\hat{H}_S - \mu \hat{N}_S)} \}. \quad (1)$$

The occupation probability of any system eigenstate reads $\rho_n = (1/Z_S) e^{-\beta(E_n - \mu N_n)}$, where states associated with the same fermion number, $N_n = N$, therefore belong to a subspace with a Boltzmann distribution $\rho_n = (e^{\beta \mu N} / Z_S) e^{-\beta E_n}$.

Interestingly, Boltzmann subspaces emerge (approximately, at least) also in nonequilibrium situations. To demonstrate this, we initially study an analytically solvable model of a noninteracting system of fermions (setting, $\forall i, j, k, l: w_{ijkl} = 0$) in the absence of coupling to bosons ($\{j_{n_b}(E)\} \equiv 0$). In the steady state the occupation probability of the \mathbf{n} th many-body eigenstate (occupation vector) reads [41]

$$P_{\mathbf{n}}^{(st)} = \prod_{m=1}^M P_{m, n_m}; \quad P_{m, n_m} = \sum_{K \in R, L} \gamma_{m, K} [(f_{K, m})^{n_m} + (n_m - 1)(f_{K, m})^{(1 - n_m)}]. \quad (2)$$

Namely, a product of orbital occupation probabilities, with $\gamma_{m, K} = |\lambda_{m, K}|^2 \Gamma_K(\varepsilon_m) / \sum_{K' \in R, L} |\lambda_{m, K'}|^2 \Gamma_{K'}(\varepsilon_m)$. Using graph theory [64–66] we show (see Supplemental Material [67]) that Eq. (2) reflects the fact that the nonequilibrium steady state satisfies an effective detailed balance condition that emerges if one lumps together the transitions of both reservoirs.

As a concrete example we consider a linear chain model of M sites, with no interactions, $\hat{H}_S = \sum_{n=1}^M E_n \hat{d}_n^\dagger \hat{d}_n + \sum_{n=1}^{M-1} t (\hat{d}_{n+1}^\dagger \hat{d}_n + \hat{d}_n^\dagger \hat{d}_{n+1}) = \sum_{m=1}^M \varepsilon_m \hat{a}_m^\dagger \hat{a}_m$. Here $\hat{d}_n^\dagger = \sum_{m=1}^M u_{n, m}^* \hat{a}_m^\dagger$ creates an electron at the n th site, \mathbf{u} is the

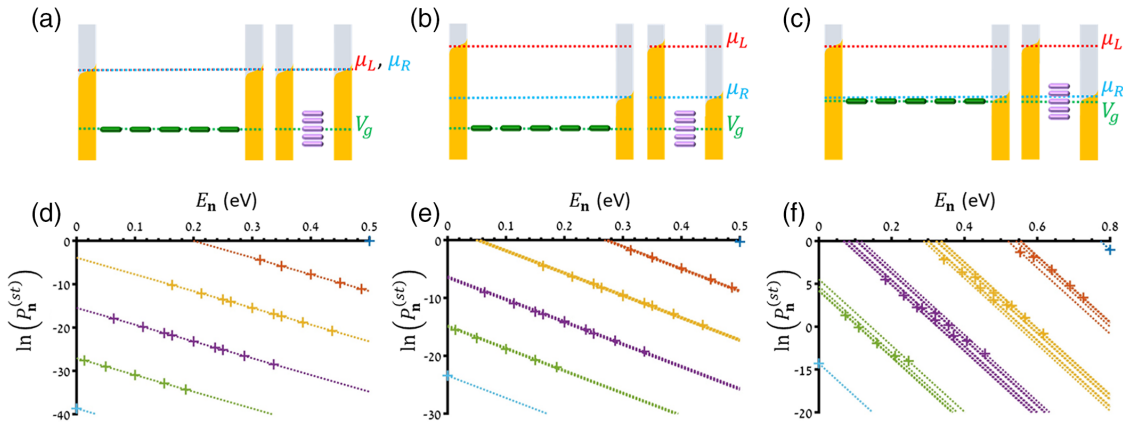


FIG. 1. Three scenarios in a molecular junction: equilibrium (a),(d), near equilibrium (b),(e), and far from equilibrium (c),(f). (a)–(c) Site (green), orbital (purple), and electrode chemical potential (dotted) energies. (d)–(f) Steady-state populations (pluses). Each state (point) is associated with a “Boltzmann line,” $\ln(P^{(st)}) = A_n - \beta E$, with $\beta = 38 \text{ 1/eV}$. States of different total electron number are colored differently. The model parameters in (a),(d) are $E_0 = 0.1$, $t = -0.05$, $\mu_L = \mu_R = 0.3$, in (b),(e) the changes are $\mu_L = 0.4$, $\mu_R = 0.2$, and in (c),(f) the additional change is $E_0 = 0.16$ (all in eV).

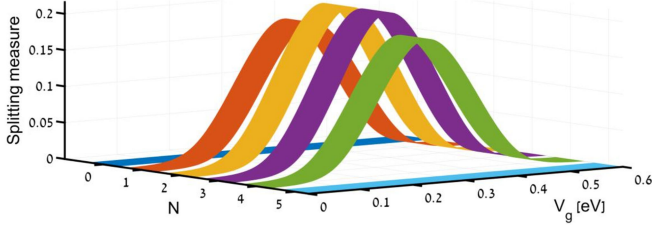


FIG. 2. Splitting measure of the Boltzmann subspaces studied in Figs. 1(c) and 1(f), where E_0 is replaced by a gate voltage, V_g . The colors correspond to different electron numbers.

eigenvector matrix of \mathbf{H} , where $[\mathbf{H}]_{n,n'} = E_n \delta_{n,n'} + t(\delta_{n',n+1} + \delta_{n,n'+1})$, and the coupling to the leads is through the terminal sites, $\hat{V}_{L(R)} \equiv d_{1(M)}^\dagger$, where $\lambda_{m,L(R)} = u_{1(M),m}^*$. For a uniform chain ($E_n \equiv E_0$), symmetry imposes $|\lambda_{m,L}|^2 = |\lambda_{m,R}|^2$. Invoking additionally the wide band limit, $\Gamma_L(\epsilon) = \Gamma_R(\epsilon) \equiv \Gamma$, we obtain $\gamma_{m,R} = \gamma_{m,L} = 1/2$.

Steady state populations of the many-body eigenstates for this model, as presented in Fig. 1, reveal clustering into Boltzmann subspaces. In or near equilibrium the states in each cluster have the same total electron number, $N_{\mathbf{n}} = N$, where the number of clusters equals $M + 1$. Importantly, the division into clusters persists even far from equilibrium. However, the number of clusters increases, namely “large” clusters split into smaller ones. To quantify this we define, $\ln(P_{\mathbf{n}}^{(st)}) + \beta E_{\mathbf{n}} = A_{\mathbf{n}}$, and consider the distribution of $\{A_{\mathbf{n}}\}$. In equilibrium the group of states associated with the same occupation number ($N_{\mathbf{n}}$) have the same $A_{\mathbf{n}}$. Otherwise, the distribution of $A_{\mathbf{n}}$ within each group broadens. The group standard deviation divided by the typical “distance” between neighboring groups ($|A_{\mathbf{n} \in N_{\mathbf{n}}} - A_{\mathbf{n} \in N_{\mathbf{n} \pm 1}}| \cong \beta(\mu_L + \mu_R)/2$) defines a splitting measure, $[2/(\beta(\mu_L + \mu_R))] \sqrt{\langle A_{\mathbf{n}}^2 \rangle - \langle A_{\mathbf{n}} \rangle^2}$. In Fig. 2 this measure

is presented for the uniform chain subject to a gate voltage, V_g . The splitting is shown to increase as the molecular orbitals penetrate the Fermi conductance window [Figs. 1(c) and 1(f)], reaching a maximum where all the orbital energies are inside. Interestingly, smaller subgroups of Boltzmann subspaces can still be identified.

The existence of Boltzmann subspaces in nonequilibrium as observed in Figs. 1 and 2 can be readily rationalized. When each orbital energy is “thermally isolated” from the lead chemical potentials ($|\epsilon_m - \mu_K| \gg k_B T$, as often holds in realistic cases), the numbers of orbitals below, inside and above the Fermi window can be identified and marked as M_b , M_w , and M_a , respectively ($M_a + M_w + M_b = M$). Using Eq. (2) with $\gamma_{m,R} = \gamma_{m,L} = 1/2$ we obtain (see Supplemental Material [67]) $P_{\mathbf{n}}^{(st)} = c_{\mathbf{n}} [N_a(\mathbf{n}), N_b(\mathbf{n}), n_{M_b+1}, n_{M_b+2}, \dots, n_{M_b+M_w}] e^{-E_{\mathbf{n}}/(k_B T)}$, where interestingly, states associated with the same total occupation numbers, below ($\sum_{m \in M_b} n_m = N_b(\mathbf{n})$) and above ($\sum_{m \in M_a} n_m = N_a(\mathbf{n})$) the Fermi window, and the same orbital occupation numbers inside the window ($\{n_m\}; m \in M_w$), share the same coefficient ($c_{\mathbf{n}}$) and are therefore a Boltzmann subspace. The number of states within each subspace depends on the different possible arrangements of N_b and N_a electrons in the orbitals below and above the conductance window. This number increases (and the number of distinctive subspaces decreases), as more orbital energies are external to the Fermi window [68], which explains the observations in Fig. 2. This central result shows that it is possible to associate physical meaning to the Boltzmann subspaces.

Allowing for disorder in the system (e.g., a nonuniform chain) or in the lead spectral densities (e.g., beyond the wide band limit) would generally result in $\{\gamma_{m,R}\} \neq \{\gamma_{m,L}\}$. Importantly, while the identification of Boltzmann subspaces is not strict in these cases, our

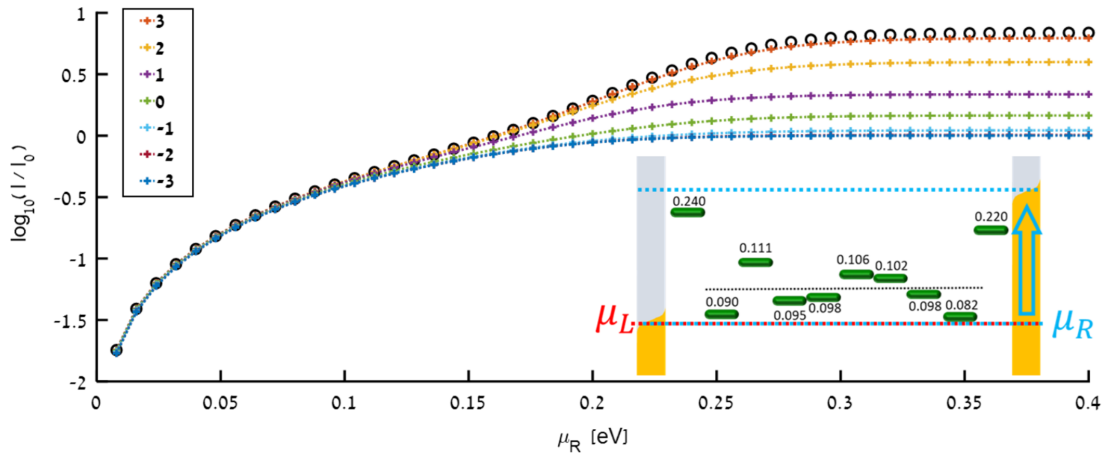


FIG. 3. Steady-state currents as functions of μ_R (for $\mu_L = 0$), in units of the maximal elastic current (I_0). Circles: Boltzmann subspaces-based calculations. Colored pluses: full calculations at different couplings to bosonic reservoirs with $\log_{10}(\Gamma_B/\Gamma) \in \{3, 2, 1, 0, -1, -2, -3\}$ (see legend) and $\hbar\omega_B = 0.15$ eV. Inset: illustration of the model with the on-site energy values marked in eV.

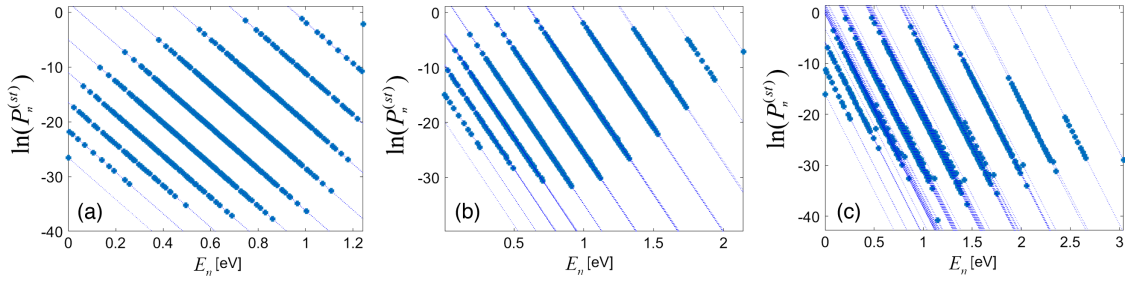


FIG. 4. Steady-state probability distributions ($\ln(P_n^{(st)})$ vs E_n) for the model presented in Fig. 3, at high bias ($\mu_R = 0.4$, $\mu_L = 0$ eV) and strong coupling to bosonic baths [$\log_{10}(\Gamma_B/\Gamma) = 3$]. (a), (b), and (c) correspond to increasing Coulomb interaction, $U = 0, 0.1, 0.2$ eV, respectively.

simulations reveal distinctive subspaces also in the presence of weak disorder or symmetry breaking (see Supplemental Material [67]).

To demonstrate that Boltzmann subspaces are useful in more general setups, we introduce coupling to bosonic reservoirs. In the realm of molecular junctions, the latter can account for molecular vibrations [69,70] or nuclear dynamics in the leads [71]. In Fig. 3 we present current-voltage curves calculated for a disordered chain of $M = 10$ sites, each coupled to a local bath with $\hat{V}_{n_b} = d_{n_b}^\dagger d_{n_b}$, and an Ohmic spectral density, $J_{n_b}(\hbar\omega) = 4\pi\Gamma_B e^{-\omega/\omega_B} \omega/\omega_B$, where ω_B and Γ_B denote the cutoff frequency and coupling energy. The calculations show that at high bias the current through the junction increases significantly with Γ_B , reflecting the opening of additional inelastic transport channels [61]. The results are compared to a reduced calculation, in which system eigenstates having the same electron occupation numbers are associated with distinctive Boltzmann subspaces. The reduced calculation qualitatively reproduces the increase in current, and even matches it quantitatively, as Γ_B increases. This can be expected, since strong coupling leads to time-scale separation, in which equilibration with the bosonic baths becomes much faster than charge transfer events. Importantly, this argument applies also to systems of interacting electrons. Adding Coulomb interactions between neighboring sites, $\hat{H}_{\text{int}} = U \sum_{n=2}^M d_n^\dagger d_n d_{n-1}^\dagger d_{n-1}$, namely, $w_{ijkl} = 2U \sum_{n=2}^M u_{n,i}^* u_{n,k} u_{n-1,j}^* u_{n-1,l}$, the system Hamiltonian no-longer commutes with the orbital number operators. The eigenstates are superpositions of different occupation vectors and the expressions for the transition rates change accordingly. Remarkably, Boltzmann subspaces can still be clearly identified (see Fig. 4) even when the interaction induces significant changes to the steady state.

Notice that in the complementary limit of zero coupling to bosonic reservoirs, a different choice of subspaces can be identified, as analyzed above for $U = 0$ and also for a concrete model with $U \neq 0$ (see Supplemental Material [67] for graph theory analysis including Refs. [72,73]). The identification of useful Boltzmann subspaces in the case of

intermediate interaction with bosonic reservoir remains an open problem.

Remarkably, as Γ_B increases the Boltzmann subspace-based calculations provide a qualitative description at a significantly smaller computational cost. For a system with $M \gg 1$ orbitals, the computational bottleneck in the exact calculation is the solution of the homogeneous master equation, scaling asymptotically as $\propto 2^{2M} M^2$. In contrast, the bottleneck in the Boltzmann subspace-based calculations is the construction of the (sparse) rate matrix which scales asymptotically only as $\propto 2^M M$, yielding an overall exponential gain (see Supplemental Material [67]). Additionally, the storage requirements for the steady state vector reduces by $[2^M/(M+1)]$, since the distribution within each subspace is analytically known. These computational advantages are expected to be even more important when the transport involves molecular network of increasing complexity [61,74–79].

In summary, the emergence of Boltzmann subspaces far from equilibrium is useful for reducing the numerical effort needed to describe steady states of complex open quantum systems. In the characteristic example of molecular junctions, we could identify Boltzmann subspaces even far from equilibrium, and even in the presence of weak disorder, interactions with bosonic reservoirs and electron-electron interactions. This phenomenon can be readily understood in scenarios where fast equilibrium is reached in subspaces separated by slow transitions, as encountered when fermion transitions were coupled to molecular vibrations. However, even in the absence of timescale separation (e.g., in the absence of coupling to the bosonic reservoirs) the equilibriumlike structure is shown to emerge when two Fermion reservoirs are merged into an effective single reservoir (see Supplemental Material [67]).

S. R. is grateful for support from the Israel Science Foundation (Grant No. 1929/21). U. P. is grateful for support from the Israel Science Foundation (Grant No. 2256/22) and Binational Science Foundation (Grant No. 2020327).

- [1] H. Spohn and J. L. Lebowitz, *Adv. Chem. Phys.* **38**, 109 (1978).
- [2] S. Hershfield, *Phys. Rev. Lett.* **70**, 2134 (1993).
- [3] C. Jarzynski, *Nat. Phys.* **11**, 105 (2015).
- [4] H. Ness, *Entropy* **19**, 158 (2017).
- [5] A. Levy, E. Rabani, and D. T. Limmer, *Phys. Rev. Res.* **3**, 023252 (2021).
- [6] G. Kurizki and A. G. Kofman, *Thermodynamics and Control of Open Quantum Systems* (Cambridge University Press, Cambridge, England, 2022).
- [7] M. Ratner, *Nat. Nanotechnol.* **8**, 378 (2013).
- [8] P. Gehring, J. M. Thijssen, and H. S. van der Zant, *Nat. Rev. Phys.* **1**, 381 (2019).
- [9] M. Thoss and F. Evers, *J. Chem. Phys.* **148**, 030901 (2018).
- [10] H. Chen, C. Jia, X. Zhu, C. Yang, X. Guo, and J. F. Stoddart, *Nat. Rev. Mater.* **8**, 165 (2023).
- [11] J. C. Cuevas and E. Scheer, *Molecular Electronics: An Introduction to Theory and Experiment* (World Scientific, Singapore, 2010).
- [12] M. Kamenetska, M. Koentopp, A. C. Whalley, Y. S. Park, M. L. Steigerwald, C. Nuckolls, M. S. Hybertsen, and L. Venkataraman, *Phys. Rev. Lett.* **102**, 126803 (2009).
- [13] W. Lee, S. Louie, A. M. Evans, N. M. Orchanian, I. B. Stone, B. Zhang, Y. Wei, X. Roy, C. Nuckolls, and L. Venkataraman, *Nano Lett.* **22**, 4919 (2022).
- [14] O. Shein-Lumbroso, J. Liu, A. Shastry, D. Segal, and O. Tal, *Phys. Rev. Lett.* **128**, 237701 (2022).
- [15] T. Yelin, R. Korytár, N. Sukenik, R. Vardimon, B. Kumar, C. Nuckolls, F. Evers, and O. Tal, *Nat. Mater.* **15**, 444 (2016).
- [16] S. Tewari, C. Sabater, and J. van Ruitenbeek, *Nanoscale* **11**, 19462 (2019).
- [17] C. Jia *et al.*, *Science* **352**, 1443 (2016).
- [18] Z. Ioffe, T. Shamai, A. Ophir, G. Noy, I. Yutsis, K. Kfir, O. Cheshnovsky, and Y. Selzer, *Nat. Nanotechnol.* **3**, 727 (2008).
- [19] Z. Wang *et al.*, *Proc. Natl. Acad. Sci. U.S.A.* **119**, e2122183119 (2022).
- [20] S. Ballmann, R. Härtle, P. B. Coto, M. Elbing, M. Mayor, M. R. Bryce, M. Thoss, and H. B. Weber, *Phys. Rev. Lett.* **109**, 056801 (2012).
- [21] L. Xiang, J. L. Palma, Y. Li, V. Mujica, M. A. Ratner, and N. Tao, *Nat. Commun.* **8**, 14471 (2017).
- [22] Y. Li, P. Doak, L. Kronik, J. B. Neaton, and D. Natelson, *Proc. Natl. Acad. Sci. U.S.A.* **111**, 1282 (2014).
- [23] J. Liu and D. Segal, *Nano Lett.* **20**, 6128 (2020).
- [24] G. Li, M. S. Shishodia, B. D. Fainberg, B. Apter, M. Oren, A. Nitzan, and M. A. Ratner, *Nano Lett.* **12**, 2228 (2012).
- [25] H. Kirchberg, M. Thorwart, and A. Nitzan, *J. Phys. Chem. Lett.* **11**, 1729 (2020).
- [26] R. Härtle, M. Butzin, O. Rubio-Pons, and M. Thoss, *Phys. Rev. Lett.* **107**, 046802 (2011).
- [27] D. Gelbwaser-Klimovsky, A. Aspuru-Guzik, M. Thoss, and U. Peskin, *Nano Lett.* **18**, 4727 (2018).
- [28] F. Chen, G. Cohen, and M. Galperin, *Phys. Rev. Lett.* **122**, 186803 (2019).
- [29] K. Miwa, A. M. Najarian, R. McCreery, and M. Galperin, *J. Phys. Chem. Lett.* **10**, 1550 (2019).
- [30] A. Baratz, A. J. White, M. Galperin, and R. Baer, *J. Phys. Chem. Lett.* **5**, 3545 (2014).
- [31] A. Borges, J. Xia, S. H. Liu, L. Venkataraman, and G. C. Solomon, *Nano Lett.* **17**, 4436 (2017).
- [32] H. K. Yadalam, S. Mukamel, and U. Harbola, *J. Phys. Chem. Lett.* **11**, 1762 (2020).
- [33] R. Volkovich, R. Härtle, M. Thoss, and U. Peskin, *Phys. Chem. Chem. Phys.* **13**, 14333 (2011).
- [34] R. J. Preston, V. F. Kershaw, and D. S. Kosov, *Phys. Rev. B* **101**, 155415 (2020).
- [35] D. Zhang, X. Zheng, and M. Di Ventra, *Phys. Rep.* **830**, 1 (2019).
- [36] C. A. Stafford, *Phys. Rev. B* **93**, 245403 (2016).
- [37] R. Härtle, C. Schinabeck, M. Kulkarni, D. Gelbwaser-Klimovsky, M. Thoss, and U. Peskin, *Phys. Rev. B* **98**, 081404 (2018).
- [38] R. J. Preston, T. D. Honeychurch, and D. S. Kosov, *J. Chem. Phys.* **153**, 121102 (2020).
- [39] C. Hsieh, J. Liu, C. Duan, and J. Cao, *J. Phys. Chem. C* **123**, 17196 (2019).
- [40] H. P. Breuer and F. Petruccione, *The Theory of Open Quantum Systems* (Oxford University, New York, 2002).
- [41] U. Peskin, *Quantum Mechanics in Nanoscience and Engineering* (Cambridge University Press, Cambridge, England, 2023).
- [42] U. Weiss, *Quantum Dissipative Systems* (World Scientific, Singapore, 2012).
- [43] G. Schaller, *Open Quantum Systems Far from Equilibrium* (Springer, Berlin, 2014), Vol. 881.
- [44] G. Cohen and M. Galperin, *J. Chem. Phys.* **152**, 090901 (2020).
- [45] V. F. Kershaw and D. S. Kosov, *J. Chem. Phys.* **147**, 224109 (2017).
- [46] P. W. Anderson, *Phys. Rev.* **124**, 41 (1961).
- [47] T. Holstein, *Ann. Phys. (N.Y.)* **29**, 410 (1964).
- [48] A. Nitzan, *Chemical Dynamics in Condensed Phases: Relaxation, Transfer and Reactions in Condensed Molecular Systems* (Oxford University Press, New York, 2006).
- [49] H. Wang and M. Thoss, *J. Chem. Phys.* **119**, 1289 (2003).
- [50] C. Meier and D. J. Tannor, *J. Chem. Phys.* **111**, 3365 (1999).
- [51] U. Kleinekathöfer, *J. Chem. Phys.* **121**, 2505 (2004).
- [52] C. Schinabeck, A. Erpenbeck, R. Härtle, and M. Thoss, *Phys. Rev. B*, **94**, 201407 (2016).
- [53] L. Mühlbacher and E. Rabani, *Phys. Rev. Lett.* **100**, 176403 (2008).
- [54] H. T. Chen, G. Cohen, and D. R. Reichman, *J. Chem. Phys.* **146**, 054105 (2017).
- [55] L. Magazzù and M. Grifoni, *Phys. Rev. B* **105**, 125417 (2022).
- [56] M. Cirio, P.-C. Kuo, Y.-N. Chen, F. Nori, and N. Lambert, *Phys. Rev. B* **105**, 035121 (2022).
- [57] G. McCaul, K. Jacobs, and D. I. Bondar, *Phys. Rev. Res.* **3**, 013017 (2021).
- [58] M. Xu, Y. Yan, Q. Shi, J. Ankerhold, and J. T. Stockburger, *Phys. Rev. Lett.* **129**, 230601 (2022).
- [59] X. Dan, M. Xu, J. T. Stockburger, J. Ankerhold, and Q. Shi, *Phys. Rev. B* **107**, 195429 (2023).
- [60] U. Peskin, *J. Phys. B* **43**, 153001 (2010).
- [61] M. Iv and U. Peskin, *J. Chem. Phys.* **152**, 184112 (2020).
- [62] H. Chen and J. Fraser Stoddart, *Nat. Rev. Mater.* **6**, 804 (2021).

- [63] A. P. Schenning and E. W. Meijer, *Chem. Commun. (Cambridge)* **26**, 3245 (2005).
- [64] T. L. Hill, *J. Theor. Biol.* **10**, 442 (1966).
- [65] J. Schnakenberg, *Rev. Mod. Phys.* **48**, 571 (1976).
- [66] F. P. Kelly, *Reversibility and Stochastic Networks* (Cambridge University Press, Cambridge, England, 2011).
- [67] See Supplemental Material at <http://link.aps.org/supplemental/10.1103/PhysRevLett.132.110401> for graph-based derivation of Eq. (2), analytic identification of Boltzmann subspaces in several systems (including in the presence of disorder, symmetry-breaking and electron-electron interactions) and demonstration of the numerical advantages of Boltzmann subspace-based calculations.
- [68] Notice that in the equilibrium case [Figs. 1(a) and 1(d)] corresponding to all orbital energies “well below” $\mu_L = \mu_R$, we have $c_{\mathbf{n}} \cong e^{\sum_{m=1}^{M_b} \epsilon_m / (k_B T)}$. In this case Eq. (3) associates the fully occupied state, $\mathbf{n} = (1, 1, \dots, 1)$, with a unit probability $P_{(1,1,\dots,1)} = c_{(1,1,\dots,1)} e^{-E_{(1,1,\dots,1)} / (k_B T)} = 1$, which means that this is the only occupied state in this scenario.
- [69] M. Galperin and A. Nitzan, *Phys. Chem. Glasses, Eur. J. Glass Sci. Technol. B* **117**, 4449 (2013).
- [70] A. Mitra, I. Aleiner, and A. J. Millis, *Phys. Rev. B* **69**, 245302 (2004).
- [71] U. Peskin, *J. Chem. Phys.* **151**, 024108 (2019).
- [72] C. S. Yang, J. F. Wang, J. Y. Lee, and E. T. Boesch, *IEEE Trans. Circuit Syst.* **35**, 1175 (1988).
- [73] M.-H. Wu and L.-Y. Chung, *Math. Prob. Eng.* **2014**, 750618 (2014).
- [74] C.-T. Shih, S. Roche, and R. A. Römer, *Phys. Rev. Lett.* **100**, 018105 (2008).
- [75] D. Brisker-Klaiman and U. Peskin, *J. Phys. Chem. C* **114**, 19077 (2010).
- [76] T. Simon, D. Brisker-Klaiman, and U. Peskin, *Advances in Quantum Methods and Applications in Chemistry, Physics, and Biology* (Springer, New-York, 2013), pp. 361–372.
- [77] H. Kim and D. Segal, *J. Chem. Phys.* **146**, 164702 (2017).
- [78] R. Korol and D. Segal, *J. Phys. Chem. B* **123**, 2801 (2019).
- [79] F. Lai Liang and D. Segal, *J. Chem. Phys.* **157**, 104106 (2022).